Pharmacokinetic Prodrug Modeling: *In Vitro* and *In Vivo* Kinetics and Mechanisms of Ancitabine Bioconversion to Cytarabine

LEE E. KIRSCH * **and ROBERT E. NOTARI** ˣ

Received November 22, 1982, from the *Lloyd M. Parks Hall, College of Pharmacy, The Ohio State University, Columbus, OH 43210.* Accepted for publication April 18, 1983. *Present address: Product Development Division, Eli Lilly and Company, Indianapolis, IN 46206.

Abstract □ Conversion rates of the prodrug ancitabine to the antileukemic cytarabine have been measured *in vivo* (rabbits) and *in vitro* (in the presence of rabbit blood and human red blood cells, blood, and plasma) using HPLC analyses for the prodrug, drug, and its inactive metabolite, 1-β-D-arabinosyluracil. These observed pH-dependent *in vitro* rate constants were consistent with those for chemical hydrolysis determined from controls using Tris buffers. Hydrolysis of ancitabine to cytarabine is chemically, not enzymatically, mediated. The blood concentration–time course for administered compound was described by a two-compartment open model following a rapid intravenous injection of prodrug, drug, or metabolite in each of three rabbits. The *in vivo* conversion rate constant (k_c) following a rapid intravenous prodrug injection was estimated by simultaneous nonlinear regression of ancitabine and cytarabine blood concentration–time courses using equations for two-compartment prodrug and drug with all possible models describing potential conversion sites. The best fit was obtained for the case allowing simultaneous conversion of the prodrug in both central and peripheral compartments to the drug in the central compartment with a common value for k_c. The resulting k_c value (0.09 h^{-1}, three rabbits) is similar to that for chemical hydrolysis (0.07 h^{-1}) at 38.8°C. Reasons why this agreement is regarded as fortuitous are discussed.

Keyphrases □ Ancitabine—bioconversion to cytarabine, mechanism, *in vivo* and *in vitro* pharmacokinetics □ Prodrug modeling—pharmacokinetics of ancitabine bioconversion to cytarabine *in vivo* and *in vitro*, mechanism □ Pharmacokinetics—prodrug modeling, ancitabine bioconversion to cytarabine *in vivo* and *in vitro*, mechanism

Ancitabine (I) has shown promise as a prodrug of the antileukemic agent, cytarabine (II) in Phase 1 (1, 2) and limited Phase 2 (2) clinical trials in the treatment of human neoplasms which respond to treatment with II. It is resistant to cytidine deaminase which rapidly inactivates II (3–5) to 1-β-D-arabinosyluracil (III) (Scheme I). In theory, the advantage of this prodrug would be to extend the biological duration of cytarabine through rate-limiting conversion (6). However, the acceptability of I is limited by acute vascular instability and parotid pain which have occurred at therapeutic doses (2).

The bioconversion mechanism of I was reported to be chemically rather than enzymatically mediated (7, 8). However, these studies report some striking dissimilarities in observed reversal rates. Wang *et al.* (7) reported 50% conversion of I to II within 6 h in mouse plasma while Ho (8) reported 45–93%, 40–55%, and 43% conversion within 1 h in human, dog, and mouse plasma. Thus, the first-order rates for hydrolysis of I based on the data reported by Ho were ~5–20 times faster than that based on data of Wang *et al.* (7). Despite this, both reports concluded that prodrug reversal was chemically mediated based on the observation that preboiling the plasma resulted in little or no decrease in hydrolysis rates.

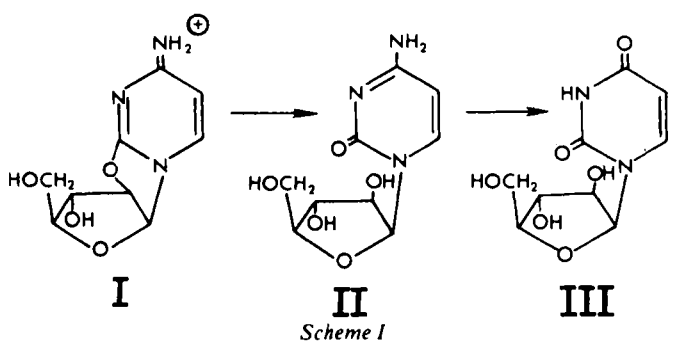

Scheme I

An *in vitro* first-order hydrolysis rate constant derived from the data of Ho was employed in a physiological pharmacokinetic model (9). The first-order hydrolysis rate constant value of 0.3 h^{-1}, which may be calculated from data presented by Ho in Fig. 6 (8) for *in vitro* hydrolysis in human plasma, did not describe the human blood concentration–time course for I and II as well as did the value 0.6 h^{-1}. This was taken as evidence that *in vivo* hydrolysis is somewhat faster than that seen *in vitro* (9).

The goals of the present study were: (*a*) to compare the conversion rates of I in blood and plasma with those predicted from aqueous hydrolysis kinetics, (*b*) to estimate the value of the *in vivo* conversion constant using classical pharmacokinetic modeling, and (*c*) to compare the observed and predicted conversion rates with those previously reported.

EXPERIMENTAL

Analytical Methods -A previously reported UV differential assay was used to measure the conversion of I to II in aqueous Tris buffers (10). Biological samples were assayed using reverse-phase HPLC. A fixed-wavelength UV detector and 20-μL sample injector loop were used in conjunction with a 3-cm precolumn and 15-cm analytical column[1]. Sodium heptanesulfonate was used as an ion-pairing agent, and *p*-hydroxybenzoic acid was the internal standard.

Cells were separated from plasma by centrifugation[2]. Plasma proteins were precipitated with 40 μL of 20% trichloroacetic acid/0.25 mL of plasma. The precipitate was removed by centrifugation, and the supernatant was filtered using a microfilter with a 0.2-μm cellulose filter membrane[3]. The filtered samples were assayed using one of three mobile phases at a flow rate of 1.2 mL/min. System A was 0.01 M acetic acid, 0.001 M sodium acetate, 0.005 M sodium heptanesulfonate, and 6% v/v methanol; the detection wavelength was 254 nm. System B was the same except that sodium acetate was 0.01 M. System C was identical to B except that 1% v/v methanol was used, and the detection wavelength was 280 nm.

The HPLC columns were preequilibrated with mobile phase for 12–24 h. Calibration curves were prepared daily from biological fluids spiked with known concentrations of I, II, III, and the internal standard. Two linear plots of peak height ratios *versus* the known concentrations were prepared for each compound in the ranges of 10^{-6}–10^{-4} and 10^{-4}–5×10^{-3} M.

***In Vitro* Kinetic Studies**—Tris buffers were prepared by weighing the free base and hydrochloride salt into double-distilled deionized water to give solutions of the following molar concentrations (base/acid): 0.016/0.084, 0.061/0.0388, and 0.085/0.0156. Sodium chloride was added to adjust the ionic strength to 0.15, which is the approximate value for plasma (11). Reaction solutions were maintained in closed water-jacketed beakers at 38°C, which is between the normal body temperature of humans (37°C) and rabbits (38.8°C) (12). Reactions were initiated by introducing an aliquot of a stock

[1] Model 332 Beckman Gradient Liquid Chromatograph with Model 153 Analytical Detector and Altex Ultrasphere-octyl 5-μm column (15 cm × 4.6 mm i.d.); Beckman Instruments, Inc., Irvine, Calif.
[2] Eppendorf Centrifuge, Model 5412; Brinkman Instruments, Westbury, N.Y.
[3] Microfilter (MF-1); Bioanalytical Systems, West Lafayette, Ind.

0022-3549/84/0600-0728$01.00/0

Table I—Concentrations of I, II, and III in Blood Resulting from an Intravenous Bolus Dose of I (3.8×10^{-4} mol/kg) in Rabbits [a]

Rabbit	Time, h	Concentration, 10^5 M I	II	III
1	0.06	117.33	(3.43)[b]	—
	0.36	36.15	1.05	0.52
	0.57	23.66	1.13	1.02
	0.99	5.12	0.86	1.34
	1.50	2.26	0.67	1.41
	2.27	1.07	0.45	1.01
	2.78	0.84	0.58	1.37
	3.17	1.03	0.47	1.50
	4.23	0.69	0.38	1.67
	5.15	0.61	0.26	1.07
	6.00	0.38	0.24	1.07
	6.93	0.34	0.24	1.09
2	0.05	159.75	(3.72)[b]	—
	0.23	63.17	1.76	—
	0.39	42.54	1.64	—
	0.73	22.43	1.48	—
	0.92	17.12	1.52	0.65
	1.49	5.54	1.23	1.15
	2.00	—	0.74	1.20
	3.40	1.11	0.58	1.68
	4.30	0.80	0.37	1.35
	5.20	0.61	0.25	1.31
	6.10	—	0.12	0.78
3	0.08	116.26	(2.54)[b]	—
	0.27	40.13	1.74	—
	0.62	15.75	1.47	0.66
	1.00	7.11	1.56	0.93
	1.49	1.95	1.26	1.20
	2.00	0.99	1.06	1.16
	3.42	0.46	0.90	1.32
	4.13	—	0.88	2.46
	5.02	0.36	0.72	2.07
	5.85	—	0.70	1.69
	6.57	0.22	0.70	1.32

[a] Concentrations are in M and dose is mol/kg because these units, unlike mass per volume or body weight, are meaningful in considering prodrug → drug stoichiometry. [b] Data points were not used in estimating k_c as explained in the *Results*.

solution of I to give a reaction concentration of 8×10^{-4} M. Samples were removed as a function of time and quenched with 0.1 M HCl. The reaction pH was measured before and after each kinetic run.

Blood was obtained from heparinized rabbits[4] *via* venipuncture of the marginal ear vein. Human venous blood was obtained from healthy volunteers and was heparinized. Heparin solutions were freshly prepared from the sodium salt because commercially available heparin injection USP contains methyl- and ethylparabens as preservatives; the parabens were observed to degrade to the internal standard, *p*-hydroxybenzoic acid. Blood which was not immediately used was refrigerated.

Biological fluids were prepared from heparinized whole human blood which was diluted to 10, 20, and 37% v/v in isotonic phosphate buffer. Human plasma and red blood cells were obtained from heparinized blood by centrifugation. Plasma was similarly diluted in isotonic phosphate buffer to 10, 20, or 37% v/v, while cells were diluted in isotonic saline to 5, 10, and 18% v/v. Although deamination of II has not been reported in human plasma, all dilutions of biological fluids were spiked with the deaminase inhibitor tetrahydrouridine to a final concentration of 1×10^{-4} M as a precaution. Rabbit plasma and heparinized whole blood were diluted to 67% v/v with isotonic saline. One reaction rate, measured in tetrahydrouridine-spiked rabbit blood and in unspiked diluted rabbit blood, showed no apparent change.

These dilutions were maintained at 38°C in water-jacketed beakers, which were stirred and closed. Reactions were initiated by addition of a solution of I to a final concentration of $\sim 1 \times 10^{-3}$ M. Aliquots were withdrawn at appropriate time intervals. Samples of whole blood and resuspended cells were immediately chilled on ice to quench the reaction, whereas plasma was quenched with trichloroacetic acid. Samples were prepared and assayed using the aforementioned HPLC procedures. The pH values of the solutions were determined at frequent intervals.

***In Vivo* Kinetic Studies**—Rabbits[4] were weighed and placed in a restraining cage[5]. Animals were heparinized (1000 U/kg of body weight) with freshly prepared heparin in sterile normal saline. A catheter attached to a sampling port[6] filled with 0.3 mL of 0.1% (w/v) heparin in normal saline was inserted into a peripheral ear artery. A sample of blood (3–5 mL) was withdrawn *via* the catheter after first removing and discarding the heparin solution and five volumes of blood totalling 1.5 mL. This preinjection blood sample was assayed as a blank and also used to prepare the standard curves with known amounts of internal standard and I, II, and/or III. After the blank was withdrawn, 0.5 mL of 0.1% heparin was placed into the port.

For each experiment, solutions of I, II, or III in sterile normal saline were injected *via* the peripheral vein in the ear opposite to that of the arterial catheter. Samples of 0.5 mL were taken at appropriate intervals *via* the arterial catheter using the procedure outlined above for the preinjection blood samples. The samples were placed in microcentrifuge tubes[7] containing 20 μL of the internal standard solution (0.25 mg/mL) and 5 μL of 0.2 M tetrahydrouridine and kept on ice until sample preparation was initiated.

Three animals were used, each of which was given an intravenous bolus dose of I, II, and III (Tables I, II, and III) with sufficient time between experiments to prevent residual blood levels from the previous study. Samples were assayed as described above for I, II, and III.

Table II—Concentrations of II in Blood as a Function of Time from an Intravenous Bolus Dose in Rabbits

Rabbit 1[a] Time, h	Conc., 10^5 M	Rabbit 2[b] Time, h	Conc., 10^5 M	Rabbit 3[c] Time, h	Conc., 10^5 M
0.06	5.96	0.06	33.88	0.39	3.85
0.25	3.74	0.10	30.59	0.60	2.69
0.51	2.10	0.23	17.85	1.08	1.80
1.06	0.99	0.63	10.24	2.00	1.05
1.55	0.82	0.85	8.84	3.12	0.57
2.60	0.41	1.16	6.91	4.36	0.34
3.65	0.29	1.48	5.39	5.20	0.21
4.50	0.23	1.90	4.11		
5.40	0.19	2.25	3.33		
		2.48	3.37		
		2.88	3.41		
		3.35	1.68		
		4.20	1.12		
		5.00	0.72		

[a] Dose = 3.39×10^{-5} mol/kg. [b] Dose = 2.06×10^{-4} mol/kg. [c] Dose = 3.80×10^{-5} mol/kg.

RESULTS

Analytical Methods—The chromatographic characteristics of I, II, and III in the HPLC systems are summarized in Table IV. Mobile phases were varied for each compound to optimize their distance from background inter-

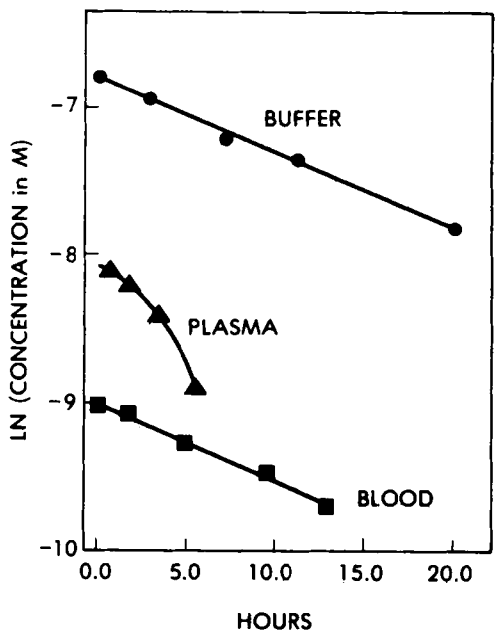

Figure 1—*First-order plots for* in vitro *conversion of I in Tris buffer (pH 7.0), diluted human blood (20% v/v), and plasma (20% v/v) at 38°C.*

[4] New Zealand White male rabbits; King's Wheel Rabbitry, Mount Vernon, Ohio.
[5] Plas-Labs, Lansing, Mich.
[6] Angiocath 22-gauge, 1 in., and PRN Adapter; the Deseret Co., Sandy, Utah.
[7] Micro test tubes, 1.5-mL polyethylene; Brinkman Instruments, Westbury, N.Y.

Table III—Concentrations of III in Blood as a Function of Time from an Intravenous Bolus Dose in Rabbits

Rabbit 1[a]		Rabbit 2[b]		Rabbit 3[c]	
Time, h	Conc., 10^4 M	Time, h	Conc., 10^4 M	Time, h	Conc., 10^4 M
0.04	2.64	0.05	3.76	0.07	3.01
0.59	1.05	0.24	2.31	0.40	1.32
1.03	0.77	0.58	1.66	0.80	1.06
1.58	0.57	1.00	1.47	1.50	0.75
2.01	0.49	1.80	1.25	2.00	0.66
3.15	0.34	3.10	1.00	3.20	0.59
4.02	0.24	4.00	0.85	4.40	0.57
5.30	0.15	5.00	0.70	5.60	0.47
6.02	0.10				

[a] Dose = 1.02×10^{-4} mol/kg. [b] Dose = 1.38×10^{-4} mol/kg. [c] Dose = 1.02×10^{-4} mol/kg.

ference, and two wavelengths (254 and 280 nm) were used to increase sensitivity. The detection ranges are given in Table IV. The lower limit of III was somewhat higher than for I or II because of background interference near the solvent front where III eluted (see capacity factors, Table IV).

During sample preparation, the treatment of plasma with trichloroacetic acid, in addition to precipitating plasma proteins, effectively quenched the conversion of I to II because I is relatively acid stable (10). This was confirmed by quantitative recovery of I from spiked plasma. Trichloroacetic acid was not added directly to blood samples because the resultant cell lysis caused unacceptable background. Instead, blood samples were kept on ice until plasma was separated by centrifugation. To test the effectiveness of the ice-bath quench, synthetic mixtures of I and II were spiked into fresh rabbit blood in concentrations similar to those observed for the first three samples of the intravenous prodrug studies (Table I) and were maintained in an ice bath for periods of time which simulated actual experimental conditions. Controls containing equivalent concentrations of I in blood and in Tris buffer (pH 7.4 at 38°C) were similarly stored. All samples were then prepared and assayed as described under *Experimental*. The mixture (1.1×10^{-3} M I, 2.5×10^{-5} M II) representing the first time point, which was stored for the longest period of 1 h, allowed <2% conversion of I to II. However, this produced a peak height for II which was 70% of those observed for the controls. Therefore, the initial assays for II (labeled as footnote b in Table I) were not used. For the remaining mixtures and storage periods, the peak heights for II in the controls were <15% of that observed in the samples. The rest of the data for II in Table I were therefore used without correction.

***In Vitro* Conversion Kinetics**—Mass balance was confirmed by the sum of the time-dependent concentrations of I and II; III was not detected in any of the reactions. Good first-order plots were obtained for reactions in Tris buffers and diluted whole blood according to:

$$\ln [I] = \ln [I_0] - k_{obs}t \qquad \text{(Eq. 1)}$$

where [I] and $[I_0]$ are the concentrations of I at time t and zero and k_{obs} is the apparent first-order conversion rate constant (Fig. 1).

First-order plots using plasma data showed significant negative deviation (Fig. 1). This was due to an increase in pH with time, thus increasing the hydroxide-ion activity (a_{OH}) which is the dominant catalytic species in aqueous solutions (10). To show that the rate in plasma was consistent with that for chemical hydrolysis, a_{OH} was calculated from measured pH and incorporated into:

$$\frac{-d[I]}{dt} = k_{OH}a_{OH}[I] \qquad \text{(Eq. 2)}$$

The resulting value for the bimolecular rate constant, k_{OH}, agreed with that observed in aqueous solutions (10).

Pharmacokinetics of II and III—The blood concentrations of II (Table II) and III (Table III) arising from rapid intravenous doses (D) of II and III were fitted using NONLIN (13) and Eq. 3:

$$C_1 = \frac{D}{V_1}\left\{\frac{(k_{21}-\alpha)}{(\beta-\alpha)}e^{-\alpha t} + \frac{(k_{21}-\beta)}{(\alpha-\beta)}e^{-\beta t}\right\} \qquad \text{(Eq. 3)}$$

which describes the time-dependent central compartment concentration (C_1) according to a two-compartment open model (Scheme II) where A1 and A2 are the amounts of drug in the central and peripheral compartments and:

$$\alpha,\beta = 0.5\{(k_{12}+k_{10}+k_{21}) \pm \sqrt{(k_{12}+k_{10}+k_{21})^2 - 4k_{21}k_{10}}\} \qquad \text{(Eq. 4)}$$

The estimated parameters are given in Table V.

Table IV—HPLC Analyses for I, II, and III in Biological Fluids

Compound	λ_{max}[a], nm	HPLC System	Capacity Factors	Detection Ranges, 10^4 M	*CV*, %[b]
I	264	A	6.8	1.0-30.0	4.0
		B	7.3	0.019-19.0	2.0
II	280	A	9.7	1.0-30.0	6.4
		C	13.7	0.010-4.0	3.9
III	260	C	4.3	0.050-4.0	6.1

[a] UV wavelength of maximum absorptivity in 0.1 M HCl. [b] Coefficient of variation is based on peak height ratios from five analyses of rabbit blood samples containing 10 μg/mL of the compound.

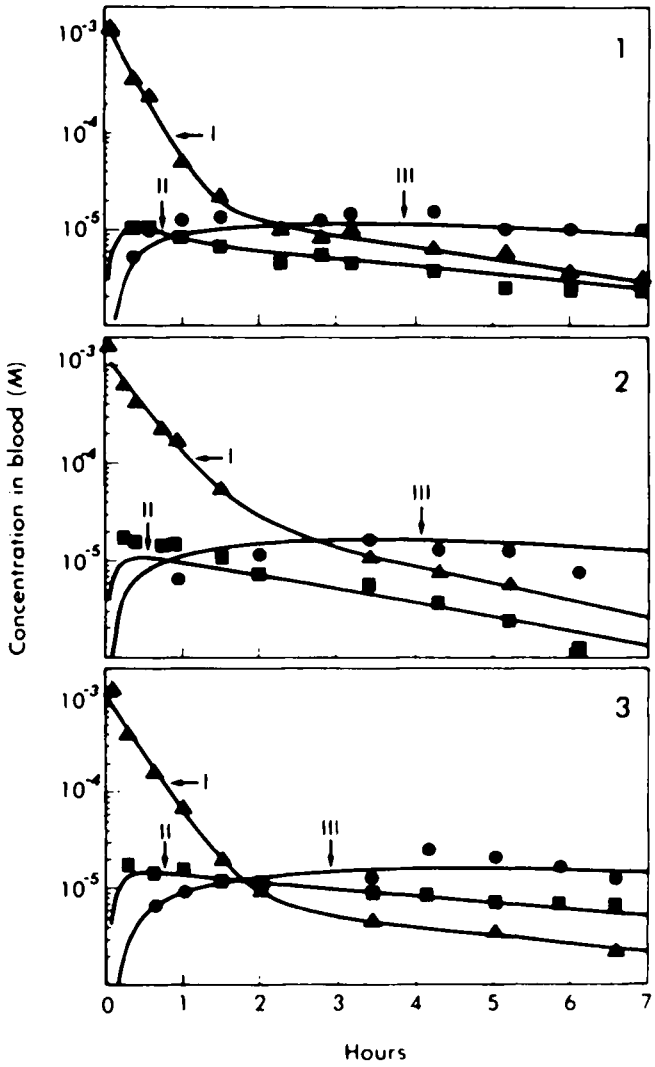

Figure 2—*Time courses for concentrations of I (▲), II (■), and III (●) following administration of 3.8 × 10^{-4}-mol/kg iv doses of I to rabbits 1, 2, and 3. Curves are based on NONLIN (13) fits using Eqs. 5, 6, and 7 for I, II, and III, as described in Scheme III.*

Prodrug Pharmacokinetics—Attempts were made to describe the blood concentrations of I and II arising from doses of I (Table I) using four different models. The elimination (k_{10}) and distribution (k_{12} and k_{21}) parameters of II were fixed at the values obtained from the NONLIN estimates using Eq. 3 following an intravenous dose of II. The elimination and distribution parameters of I (k_c, k'_{10}, k'_{12}, k'_{21}, and V'_1) were adjusted by NONLIN. The four models differed in their routes for prodrug conversion. The simplest model

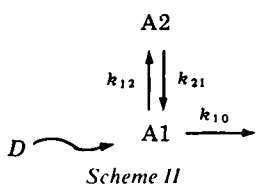

Scheme II

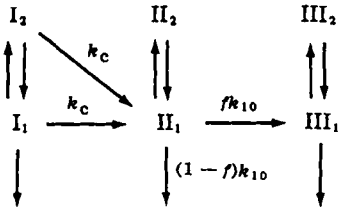

Scheme III

allowed conversion from I_1 to II_1 only. In the other models conversion was set at $I_1 \rightarrow II_1$ and $II_2 \rightarrow II_1$ (see Scheme III); $I_1 \rightarrow II_1$, $I_2 \rightarrow II_1$, and $I_2 \rightarrow II_2$; or $I_1 \rightarrow II_1$ and $I_2 \rightarrow II_2$. NONLIN fits limiting conversion to $I_1 \rightarrow II_1$ with or without $I_2 \rightarrow II_2$ consistently underestimated the concentration of II, while those using all three routes ($I_1 \rightarrow II_1$, $I_2 \rightarrow II_1$, and $I_2 \rightarrow II_2$) significantly underestimated data for the terminal phase of I_1. However, Eqs. 5–7, based on Scheme III, yielded excellent fits to the blood concentration data for I and good fits for II (Fig. 2):

$$[I] = \frac{D}{V'_1}\left\{\left[\frac{(k_c + k'_{21} - \alpha')}{(\beta' - \alpha')}\right] e^{-\alpha' t} + \left[\frac{(k_c + k'_{21} - \beta')}{(\alpha' - \beta')}\right] e^{-\beta' t}\right\} \quad \text{(Eq. 5)}$$

$$[II] = \frac{Dk_c}{V_1}\left\{\left[\frac{(k_{21} - \alpha)(k_c + k'_{21} + k'_{12} - \alpha)}{(\beta' - \alpha)(\alpha' - \alpha)(\beta - \alpha)}\right] e^{-\alpha t} + \left[\frac{(k_{21} - \beta)(k_c + k'_{21} + k'_{12} - \beta)}{(\beta' - \beta)(\alpha' - \beta)(\alpha - \beta)}\right] e^{-\beta t} + \left[\frac{(k_{21} - \beta')(k_c + k'_{21} + k'_{12} - \beta')}{(\alpha' - \beta')(\alpha - \beta')(\beta - \beta')}\right] e^{-\beta' t} + \left[\frac{(k_{21} - \alpha')(k_c + k'_{21} + k'_{12} - \alpha')}{(\beta' - \alpha')(\alpha - \alpha')(\beta - \alpha')}\right] e^{-\alpha' t}\right\} \quad \text{(Eq. 6)}$$

where α' and β' refer to I and are defined as:

$$\alpha', \beta' = 0.5\{(k'_{21} + k'_{12} + k'_{10} + 2k_c) \pm \sqrt{(k'_{21} + k'_{12} + k'_{10} + 2k_c)^2 - 4[k_c^2 + k_c(k'_{10} + k'_{12} + k'_{21}) + k'_{21}k'_{10}]}\} \quad \text{(Eq. 7)}$$

and α and β are defined in Eq. 4. Allowing unequal k_c values for conversion of $I_2 \rightarrow II_1$ and $I_1 \rightarrow II_1$ did not improve these fits.

The common method for calculating f, the fraction of II that is metabolized to III, is to determine the area under the concentration–time curve for III following an intravenous dose of II (14). Since the duration of III was long relative to I and II and the research goals did not require an accurate assessment of f, the terminal data for III were obtained only after intravenous doses of III. The observed concentration–time course for III, following an intravenous dose of I, was then described by reiterating f values in:

$$[III] = \frac{Dk'_c f k_{10}}{V_1^*}\left\{\left[\frac{(k_{21} - \alpha')(k^*_{21} - \alpha')(k_c + k'_{21} + k'_{12} - \alpha')}{(\beta' - \alpha')(\alpha - \alpha')(\beta - \alpha')(\alpha'' - \alpha')(\beta'' - \alpha')}\right] e^{-\alpha' t} + \left[\frac{(k_{21} - \alpha)(k^*_{21} - \alpha)(k_c + k'_{21} + k'_{12} - \alpha)}{(\alpha' - \alpha)(\beta' - \alpha)(\beta - \alpha)(\alpha'' - \alpha)(\beta'' - \alpha)}\right] e^{-\alpha t} + \left[\frac{(k_{21} - \alpha'')(k^*_{21} - \alpha'')(k_c + k'_{21} + k'_{12} - \alpha'')}{(\alpha' - \alpha'')(\beta' - \alpha'')(\alpha - \alpha'')(\beta - \alpha'')(\beta'' - \alpha'')}\right] e^{-\alpha'' t} + \left[\frac{(k_{21} - \beta')(k^*_{21} - \beta')(k_c + k'_{21} + k'_{12} - \beta')}{(\alpha' - \beta')(\alpha - \beta')(\beta - \beta')(\alpha'' - \beta')(\beta'' - \beta')}\right] e^{-\beta' t} + \left[\frac{(k_{21} - \beta)(k^*_{21} - \beta)(k_c + k'_{21} + k'_{12} - \beta)}{(\alpha' - \beta)(\beta' - \beta)(\alpha - \beta)(\alpha'' - \beta)(\beta'' - \beta)}\right] e^{-\beta t} + \left[\frac{(k_{21} - \beta'')(k^*_{21} - \beta'')(k_c + k'_{21} + k'_{12} - \beta'')}{(\alpha' - \beta'')(\beta' - \beta'')(\alpha - \beta'')(\beta - \beta'')(\alpha'' - \beta'')}\right] e^{-\beta'' t}\right\} \quad \text{(Eq. 8)}$$

which is based on Scheme III wherein α'' and β'' refer to III as evaluated in Eq. 3. All pharmacokinetic values were those previously obtained, while the value for f was manually adjusted between its limits, $0 \le f \le 1$. The best fits (Fig. 2), assessed by visual inspection, were obtained as f approached 1 (Table V).

DISCUSSION

***In Vitro* Conversion**—The pH–rate profile for the hydrolytic conversion of I in the temperature range of 19–80°C, at ionic strengths (μ) of 0.01–1.5 and pH values from 1 to 12 can be constructed by plotting the logarithm of the apparent first-order rate constant (k_{app}) calculated from Eq. 9 *versus* pH:

$$k_{app}\,(\text{in h}^{-1}) = 1.74 \times 10^{17}\, a_{OH} \times \exp\left\{\frac{-1.15\sqrt{\mu}}{1 + \sqrt{\mu}} - \frac{8662}{T}\right\} + 1.12 \times 10^{11} \exp\{-10121/T\} \quad \text{(Eq. 9)}$$

where T is absolute temperature. The accuracy of Eq. 9 is generally good (10). The average deviation between calculated and observed rate constants in aqueous solutions is <20%. The line in Fig. 3 represents the calculated pH–rate profile for chemical conversion at 38°C, $\mu = 0.15$, using Eq. 9. Agreement with the observed constants from studies in Tris buffers (Fig. 3) substantiates the accuracy of the predictive equation.

Each bimolecular rate constant from the three human plasma dilutions was multiplied by a_{OH} for the median pH value of the run. The logarithm of these pseudo first-order constants, together with the k_{obs} values obtained in diluted human blood, red blood cells, and rabbit blood are shown in Fig. 3 as a function of pH. These data agree with those for chemical conversion. The slight positive deviations were independent of the concentration of biological fluid and solids in the dilutions. Therefore, it is concluded that the mechanism of prodrug conversion in human and rabbit blood is chemical hydrolysis.

The results of this study were compared with those in the literature by approximating first-order conversion rate constants from reported data using:

$$k_{app} = \ln(F_r)/t_i \quad \text{(Eq. 10)}$$

where F_r is the reported fraction of $[I_0]$ remaining at the end of the incubation period, t_i. This assumes first-order kinetics and constant pH and mass balance based on [I] and [II]. Based on this study, the first and last assumptions are probably valid. The logarithms of the calculated k_{app} values are plotted in Fig. 3 at the reported pH. The data of Wang *et al.* (7) agree with the results obtained in this study, as do the Tris buffer studies of Ho (8). However the k_{app} values calculated from the biological fluid data of Ho show a large positive deviation.

An unequivocal explanation of the large positive deviation is not possible. However it is likely that chemical conversion continued after the incubation period, which would result in erroneously high rate constants. Ho employed ethanol to quench the reactions. The rate constants for conversion at room temperature in cleaned plasma (the supernatant of plasma treated with ethanol) were determined for comparison. These rate constants, shown in Fig. 3, are similar to those based on data reported by Ho, but much larger than those predicted for hydrolysis at 38°C. The methods of quenching used in this paper (acidification or chilling) were shown to be 100 and 98% effective, respectively.

***In Vivo* Conversion**—The kinetics of simultaneous hydrolysis and distribution in an isobutyl alcohol–aqueous acid two-phase transfer cell behave like the two-compartment open model shown in Scheme II (15). The time-de-

Table V—Pharmacokinetic Parameters of I, II, and III

Compound	Rabbit 1	Rabbit 2	Rabbit 3
I[a]			
k_c (h^{-1})	0.066(0.005)	0.091(0.017)	0.108(0.008)
k_{12} (h^{-1})	0.619(0.042)	0.402(0.070)	0.497(0.051)
k_{21} (h^{-1})	0.259(0.025)	0.421(0.113)	0.137(0.028)
k_{10} (h^{-1})	2.785(0.148)	1.938(0.142)	2.356(0.189)
V_1 (L/kg)	0.288(0.027)	0.301(0.031)	0.351(0.054)
CL (L/kg·h)	0.86	0.63	0.95
II[b]			
k_{12} (h^{-1})	1.063(0.212)	3.551(1.427)	1.459(0.719)
k_{21} (h^{-1})	0.633(0.122)	2.096(0.297)	1.434(0.261)
k_{10} (h^{-1})	1.433(0.167)	2.025(0.620)	1.243(0.601)
V_1 (L/kg)	0.420(0.058)	0.343(0.123)	0.413(0.218)
CL (L/kg·h)	0.60	0.69	0.51
f_c	0.06[c]	0.08[c]	0.12[c]
III[d]			
k_{12} (h^{-1})	1.675(0.361)	4.074(0.157)	2.619(0.547)
k_{21} (h^{-1})	1.635(0.219)	1.500(0.045)	0.492(0.124)
k_{10} (h^{-1})	0.780[e] (0.110)	0.746(0.027)	0.823(0.167)
V_1 (L/kg)	0.290[e] (0.050)	0.175(0.007)	0.123(0.025)
CL (L/kg·h)	0.23	0.13	0.10
f	1.0	0.9	0.9

[a] From simultaneous NONLIN fits of concentration time courses for [I] and [III] arising from an intravenous bolus dose of I (Table I). [b] From NONLIN fit of [II] time course following an intravenous bolus dose of II (Table II). [c] Based on dose-adjusted (3.8×10^{-4} mol/kg) AUC values for drug after intravenous administration of prodrug (AUC_{pd}) and drug (AUC_d) where f_c, the fraction of prodrug converted to drug, is $(AUC_{pd})/(AUC_d)$ and values (in 10^5 mol·h/kg) are: (4.1/64), (4.2/55), and (9.0/74). [d] From NONLIN fit of [III] time course arising from an intravenous bolus dose of III (Table III) except for f, which was estimated as described in the *Results*. [e] Value of NONLIN estimate after adjustment to accommodate [III] time course arising from an intravenous bolus dose of I. Reported value is within the 95% confidence interval of the original NONLIN estimate.

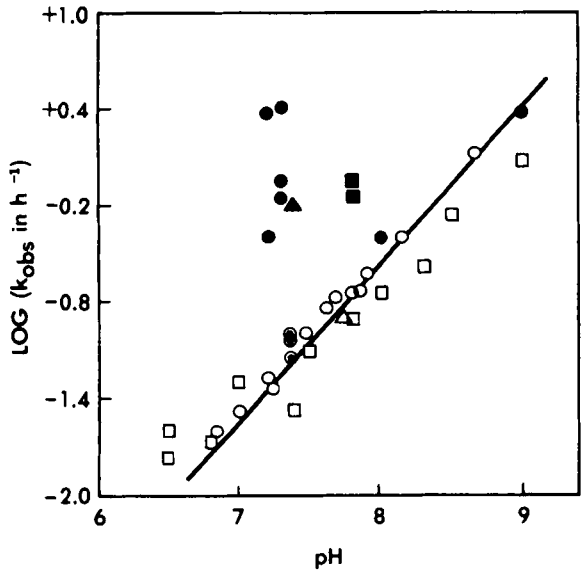

Figure 3—*The pH-rate profile for the conversion of I in rabbits (◎) and* in vitro. *The line represents chemical conversion in aqueous solution at 38°C, μ = 0.15, calculated by Eq. 9. The* in vitro *rate constants are: (○) Tris buffers, diluted human red blood cells, blood, and plasma; (△) diluted rabbit blood; (■) human plasma treated with ethanol; calculated by applying Eq. 10 to the data of (□) Wang* et al. *(7) and (●) Ho (8); (▲) applied to a physiological pharmacokinetic model by Himmelstein and Gross (9).*

pendent concentrations in the aqueous phase were described by Eq. 3, which employed the first-order rate constants for distribution (k_{12} and k_{21}) and hydrolysis (k_{10}). Hydrolysis rate constants (k_h) measured independently in aqueous acid controls agreed with the k_{10} values, which were dependent on acid concentration but independent of stirring rate, which increased k_{12} and k_{21}. Thus, the hydrolysis rate constant can be calculated from the biexponential aqueous phase data using Eq. 3 without any knowledge of the volumes in the transfer cell. The application of an *in vitro* hydrolysis rate constant to an *in vivo* classical pharmacokinetic model would require the achievement of a constant homogeneous apparent volume of distribution in a manner kinetically analogous to the transfer-cell experiments. Thus, if a chemically reversing prodrug were uniformly distributed in a fixed aqueous volume (such as extracellular fluid) with little tissue or plasma protein binding, one would expect its *in vitro* conversion constant to agree with the mechanistically related *in vivo* pharmacokinetic microconstant. *A priori*, ancitabine (I) appeared to possess the pharmacodynamic properties required to demonstrate such a correlation. It does not readily enter cells or deposit into fat (16–18) and its *in vivo* conversion is chemical hydrolysis.

It was not possible to achieve this result with data from rabbits. Although the *in vivo* conversion constants (k_c) agree with those for chemical hydrolysis (Fig. 3), the model of best fit required conversion of both I_1 and I_2 to II_1. A physiological interpretation of the resulting model (Scheme III) is not possible. The average model-independent *Vd* value for I (calculated from CL/β) is 2.9 L/kg, which is larger than that for II (1.4 L/kg) and much greater than the total body water (0.7 L/kg) for rabbits (19). Thus, one (or more) of the requirements for a meaningful correlation is absent, and the observed agreement between the *in vivo* and *in vitro* hydrolysis rate constants must be regarded as fortuitous.

In Fig. 3, the rate constant successfully used by Himmelstein and Gross (9) shows a large positive deviation from the rate constants for chemical, *in vitro* (blood), and *in vivo* (rabbit) conversion. An increased value for the *in vivo* rate constant over the initial *in vitro* estimate based on the results of Ho caused the authors to conclude that hydrolysis occurs somewhat faster *in vivo*. Another explanation for the successful prediction of concentration–time profiles of I and II in humans using high k_c estimates in the physiologically based model might be that the distribution volume for I was underestimated. Since the apparent first-order rate constant is always multiplied by the volume of the specific tissue to obtain a corresponding clearance value, an underestimate in the total volume of distribution would require an overestimate in the conversion constant in order to describe the data. The volume of distribution for I, which was unknown in humans, was assigned a value equal to that for II. The average *Vd* for I in rabbits is twice the value for II. This could explain the successful fit obtained with the high hydrolysis rate constant if the same trend holds in humans. Thus, the conclusion that *in vivo* hydrolysis is somewhat faster than hydrolysis *in vitro* was speculative. No conformatory evidence of facilitated *in vivo* conversion was found in the present study. While both the physiologically based model and the classical model described the *in vivo* data, neither was based on physiological actuality.

The hypothesis that prolonged duration of I is due to the slow hydrolytic conversion of I to II, as proposed by Ho (8) and supported by Himmelstein and Gross (9), is corroborated by the present study. The terminal half-life of II from an intravenous dose of I (Fig. 2, average $t_{0.5} \cong 5$ h) is three times that observed following an intravenous dose of II.

REFERENCES

(1) P. L. Chawla, J. J. Lokich, N. Jaffe, and E. Frei, *Proc. Am. Assoc. Cancer Res.*, **15**, 188 (1974).

(2) J. H. Burchenal, K. Kalaher, B. Clarkson, N. Kememey, C. Young, J. Fox, and I. Krakoff, *Curr. Chemother., Proc. Int. Congr. Ther., 10th*, **2**, 1206 (1978).

(3) D. H. W. Ho, C. J. K. Carter, T. L. Loo, R. L. Abbott, and C. M. McBride, *Drug Metab. Dispos.*, **3**, 309 (1975).

(4) A. Hoshi, M. Iigo, M. Saneyoshi, and L. Kurentani, *Chem. Pharm. Bull.*, **21**, 1235 (1973).

(5) W. Kreis, T. M. Woodcock, M. B. Meyers, L. A. Carlevarini, and I. H. Krakoff, *Cancer Chemother. Res.*, **61**, 723 (1977).

(6) R. E. Notari, *Pharmacol. Ther.*, **14**, 25 (1981).

(7) M. C. Wang, R. A. Sharma, and A. Bloch, *Cancer Res.*, **33**, 1265 (1973).

(8) D. H. W. Ho, *Biochem. Pharmacol.*, **23**, 1235 (1974).

(9) K. J. Himmelstein and J. F. Gross, *J. Pharm. Sci.*, **66**, 1441 (1977).

(10) L. E. Kirsch, Ph.D. Thesis, College of Pharmacy, The Ohio State University, Columbus, Ohio, 1982.

(11) E. J. Masoro, "Acid-Base Regulation: Its Physiology and Pathophysiology," W. B. Sanders, Philadelphia, Pa., 1971, pp. 3, and 30.

(12) B. M. Mitruka and H. M. Rawnsley, "Clinical Biochemical Hematological Reference Values in Normal Experimental Animals," Masson, New York, N.Y., 1977, p. 6.

(13) C. M. Metzler, G. L. Elfring, and A. J. McEwen, *Biometrics*, **30**, 3 (1974).

(14) R. E. Notari, "Biopharmaceutics and Clinical Pharmacokinetics," 3rd ed., Dekker, New York, N.Y., 1980, pp. 55, 231, and 267.

(15) E. Tomlinson, R. E. Notari, and P. R. Byron, *J. Pharm. Sci.*, **69**, 655 (1980).

(16) M. C. Wang, R. A. Sharma, and A. Bloch, *Cancer Res.*, **33**, 1265 (1973).

(17) H. Hirayama, T. Sugihara, F. Hamada, T. Kanai, J. Hikita, Y. Araki, K. Kuretani, and A. Hoshi, *Gann*, **65**, 153 (1974).

(18) S. M. ElDareer, V. M. White, K. Tillery, F. P. Chen, L. B. Mellett, and D. L. Hill, *Cancer Treat. Rep.*, **61**, 805 (1977).

(19) P. L. Altemann and D. S. Dittmer, "Biology Data Book," Federation of Americas Societies for Experimental Biology, Bethesda, Md., 1974, p. 1990.

ACKNOWLEDGMENTS

The authors gratefully acknowledge the Elsa U. Purdee Foundation, The National Institutes of Health (Predoctoral Training Grant T32GM07622-05), The Upjohn Company and its Medical Sciences Liaison, David F. Lichtenauer, for partial support of this work.